DOI: 10.61782/fa.2025.0949

FORUM ACUSTICUM EURONOISE 2025

VALIDATION STUDY OF BROADBAND NUMERICAL METHODS FOR ROOM ACOUSTIC SIMULATIONS AND BINAURAL RENDERING IN A FURNISHED ROOM

Hermes Sampedro Llopis[1*] **Steinar Guðjónsson**[1] **Matthias Cosnefroy**[1]
Haukur Hafsteinsson[1] **Finnur Pind**[1]
[1] Treble Technologies, Iceland

ABSTRACT

Previous research introduced a wave-based acoustic simulation framework, which demonstrated high-accuracy predictions of spatial room impulse responses. This study further refines the framework to enable broadband simulations across an extended frequency range up to 12 kHz. Additionally, the effect of air absorption, crucial for covering the full 8 kHz octave band, is included. The sound field is encoded into spherical harmonics using a spherical array of receivers, employing a 32nd-order ambisonics configuration. The framework utilizes these encodings to render binaural signals via a head-related transfer function, measured under anechoic conditions. Initially, the method is validated in an empty room setup model. Subsequently, a second model is considered incorporating various living room furnishings. The simulation results are compared with the measurements in situ. In both configurations, empty and furnished, the simulated binaural outputs show remarkable concordance with the measured data, highlighting the framework's efficacy in accurately replicating real-world complex acoustic environments. This enables practical applications such as simulating complex audio devices, including wearable technology, in diverse acoustic environments for preliminary testing and prototyping.

Keywords: *Broadband room acoustics simulations, numerical methods, wave-based, binaural rendering.*

**Corresponding author*: *hl@treble.tech.*

1. INTRODUCTION

Room acoustic simulations are used in different design applications, such as building design, product design, music, and entertainment. During the design stage, accuracy and efficiency are crucial. However, accuracy is generally obtained at the expense of computational efficiency. Historically, room acoustic simulations have been performed using geometric acoustic (GA) methods [1], such as ray tracing and image source, which approximate sound propagation at high frequencies to ensure a manageable computational cost. These methods are known to degrade the simulation accuracy as they fail to simulate the correct wave nature of the sound, e.g. diffraction and interference at low frequencies. Another approach is to perform simulations with wave-based methods, which solve the wave equation numerically using discretization methods [2–5]. In this case, wave phenomena are included, leading to more accurate results than GA, especially at low frequencies. However, the computational cost increases dramatically when simulating higher frequencies, introducing a challenge for design purposes. In previous work, a wave-based solver that enables accurate room acoustic simulations was presented with a framework to estimate high-order spatial impulse responses, which can be combined in postprocessing with head-related transfer functions (HRTF) to provide binaural renderings. The study showed a rectangular 80 m^3 empty room up to 8 kHz. In this study, we extended the wave-based framework to perform a validation study up to 12 kHz (covering the whole 8 kHz octave band). A similar 80 m^3 room is considered, where different living room furnishings are included. This study case demonstrates the potential and precision of the framework in complex room acoustic simulations.

2. METHODS

2.1 Theoretical background

The acoustic wave propagation in a lossless and steady medium is described by the second-order wave equation,

$$\frac{\partial^2 p}{\partial t^2} - c^2 \Delta p = 0, \tag{1}$$

where $p(\boldsymbol{r}, t)$ is the sound pressure, $\boldsymbol{r} \in \Omega$ the position in the domain $\Omega \in \mathbb{R}^3$, t is the time in the interval $[0, T]$ s and c is the speed of sound ($c = 343$ m/s). The second-order equation can also be written as a system of two coupled linear first-order partial differential equations, also called the homogeneous linearized Euler equations

$$\frac{\partial \boldsymbol{v}}{\partial t} = -\frac{1}{\rho}\nabla p, \tag{2a}$$

$$\frac{\partial p}{\partial t} = -\rho c^2 \nabla \cdot \mathbf{v}, \tag{2b}$$

where $\mathbf{v} = (v_x, v_y, v_z)$ is the particle velocity at time t and location $\mathbf{r} = (x, y, z)$, and ρ is the density of the medium ($\rho = 1.2$ kg/m^3). The system can be excited with an initial condition, for example, a Gaussian pulse with a spatial variance for the sound pressure.

The system of equations is discretized and solved using the discontinuous Galerkin Finite Element Method (DG-FEM). Both spatial and temporal operators are approximated with fourth-order accuracy. The details are omitted but can be found in previous publications, e.g., in [6–8].

In addition, air absorption of the room is included in a post-processing stage. The method was presented by Horniks et al., 2008 [9], which uses the continuous wavelet transform, with parameters described in the ISO 9613-1 standard [10].

The numerical solver provides results for the pressure and particle velocity in the time domain, where the sound field is sampled spatially using spherical arrays of virtual microphones centered on the desired listening position. This data is processed to provide a single spatial receiver that contains the high-order spatial impulse responses, which can be combined in post-processing with a device-related transfer function (DRTF) dataset to render the response, i.e. using measured HRTFs to obtain the response at the location of the ears. A detailed description of the method can be found in previous work [11] and is here omitted for brevity.

2.2 Validation experiment

In this study, validation consists of two parts. First, an empty rectangular room of 80 m^3 is considered. The room in question is made of concrete, except for a wood door. The reverberation time (RT) of the room is adjusted to 0.6 s by placing rockwool absorbers, 100 mm and 120 mm thick, on the walls and the floor. Measurements were carried out following the ISO-standard 3382 [12], where six positions were considered (two source positions and three receiver positions).

Second, the same empty room is furnished, where a large and small couch, a table, a coffee table, a bookcase, a television, and a carpet were introduced. The room model is presented in Figure 1, where a circled mark indicates the origin. Six different sources-receiver positions were considered for this study; however, only one position is presented to avoid an overload of results. The source is located at $\boldsymbol{r}_{s1} = (4.8, 0.82, 0.94)$ m and the spatial receiver at $\boldsymbol{r}_{r1} = (3.55, 3.32, 1.42)$ m with a rotation of 270°. The reference orientation is defined along the x-axis and increases in the counterclockwise direction. An additional monophonic impulse response is considered in position $\boldsymbol{r}_{r1_{mono}} = (1.283.181.44)$ m.

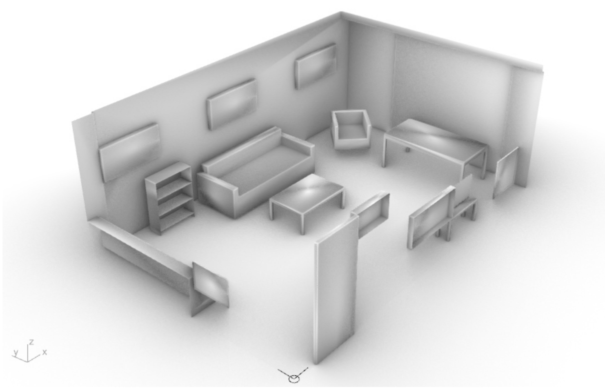

Figure 1: Furnished room setup.

The sound source utilized for the validation study is a one-way Mixcube Active Avantone speaker. For the simulations, the source is modeled from the loudspeaker's CAD file, applying a boundary velocity source at the membrane to approximate a flat piston. Monophonic room impulse responses are measured using a GRAS $1/2$-inch free-field microphone and simulated with a mono receiver. However, binaural room impulse responses are measured using a head and torso simulator (HATS). Binaural simulations are generated by first computing 32nd-order ambisonics from the spherical receiver array, then post-processed using a HATS mannequin HRTF dataset measured under anechoic conditions.

All simulations are carried out with Treble's wave-based solver, which has been optimized to allow for room acoustic simulations up to 12 kHz and the IR length corresponding to a sufficient value to ensure a 40 dB, averaged, broadband decay of the measurements. The surface impedance of the Rockwool absorbers was measured separately in an impedance tube according to ISO 10534-2, which provided valid results between 200 Hz and 2000 Hz and were extrapolated for the entire simulation spectrum [13]. The absorption properties of the remaining surfaces and objects are taken from the established databases. Measurements data are referenced to the 1 m on-axis anechoic response of the speaker, while simulations are referenced to the 1 m on-axis free-field simulation response.

3. RESULTS

3.1 Empty room

As mentioned above, the reverberation time of the empty room was adjusted to 0.6 s. The average values for $T20$ and the standard deviation of the six positions of the source-receiver pair, according to the ISO 3382 standard, are presented in Figure 2 for measurements and simulations.

The simulation results match the measurements well. The largest deviation is found to be 12% for the 4 kHz octave band. On the other hand, the smallest difference is found for the 125 Hz band with a perfect match. Assuming that the just noticeable difference (JND), described in ISO 3382 [12], is defined as a difference in reverberation time 5%, the largest deviation corresponds to 2 JNDs. In addition, the energy decay curves for both measurements and simulations are presented in Figure 3 for different frequency bands. In general, the simulated behaviour matches very closely with the measurements. Note that the curves vary depending on the source-receiver pairs, but in general, all the positions showed similar results. In both room configurations, the simulation time was found to be 20 hours running on eight A100 GPUs.

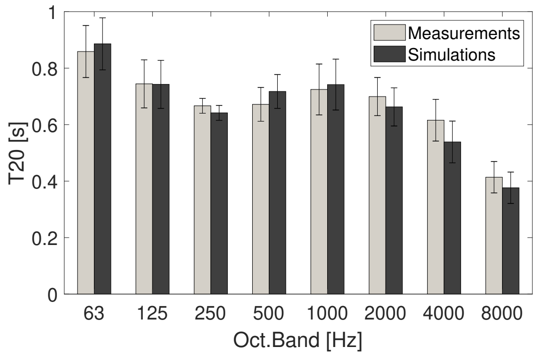

Figure 2: Averaged $T20$ over the six source-receivers pairs according to ISO-3382 for both, simulations and measurements with standard deviation.

3.2 Furnished room

For the furnished room, the mono receiver $\boldsymbol{r}_{r1_{mono}}$ is first considered. Figure 4a displays the simulated and measured room impulse responses, focusing on the initial 0.15 s to demonstrate how the simulation closely matches the measured initial reflections and the overall decay trend. Figure 4b illustrates the frequency response averaged over the $1/48^{th}$ octave bands. This averaging yields a smoother response, particularly at high frequencies, facilitating a more precise comparison between the simulated and measured responses. The simulated results demonstrate a strong correlation with the measurements, With the lower-frequency modes closely aligned and the high-frequency trends closely matching.

Second, the spatial receiver $\boldsymbol{r}_{r1}$ is considered. Figure 5a shows a comparison between measured HATS binaural impulse responses and the simulated and rendered binaural responses of the same HATS device. A good match is obtained in the time domain. All the prominent early reflections that are seen in the simulated response show a correct time of arrival and amplitude. Note that the left ear (L) faces the source, presenting an earlier arrival time and a higher amplitude than the right ear (R). In the frequency domain, presented in Figure 5b, an excellent match can be observed. Again, the spectrum is averaged over $1/48^{th}$ octave bands, and it is possible to see how the low-frequency modes match well, and the high-frequency trend is very well captured. These results are improved compared to the previous study, in which air absorption was not included, presenting higher levels of amplitude at high frequencies due to lack of absorption [11].

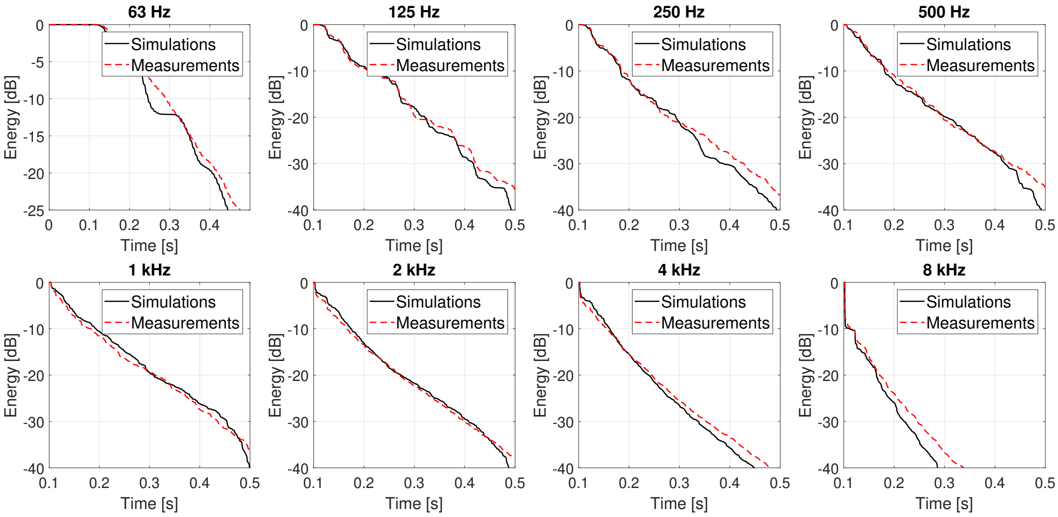

Figure 3: Comparison of measured against simulations of the Energy Decay Curves per frequency bands for one of the source-receiver pairs.

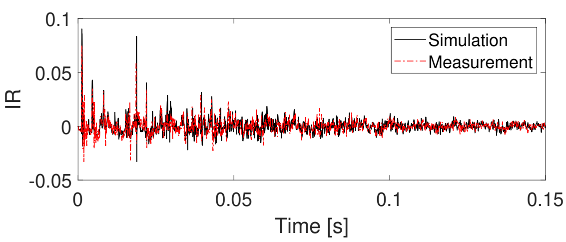

(a) Room impulse response.

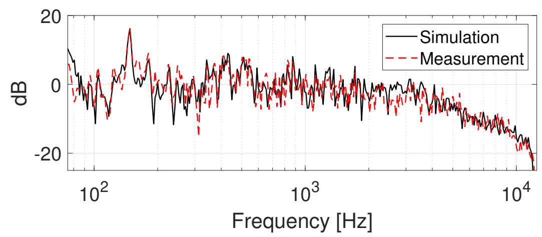

(b) Magnitude in the frequency domain.

Figure 4: Measured and simulated mono IRs in the furnished room.

4. CONCLUSION

This study validates a wave-based simulation framework, previously introduced, up to 12 kHz in the context of room acoustics. It employs physically accurate simulations of complex scenarios, specifically a rectangular, furnished room with various objects made from different materials. The simulations are rendered in post-processing to generate binaural responses from a HATS mannequin, which are then compared to in situ simulations. Notably, this approach offers the flexibility to render any device in any orientation during the post-processing stage, utilizing the results from spatial receivers. The results show a good agreement, first when comparing acoustic parameters, demonstrating the potential of using wave-based methods, where the acoustic parameters can be accurately predicted, even at low frequency bands, where GA would not have succeeded; and second, in terms of time of arrival, amplitude and frequency responses. This confirms that the framework can produce highly precise simulations for complex acoustic environments up to 12 kHz, with computation times that are feasible for design applications.

5. REFERENCES

[1] L. Savioja and U. P. Svensson, “Overview of geometrical room acoustic modeling techniques,” *The Journal of the Acoustical Society of America*, vol. 138, no. 2, pp. 708–730, 2015.

[2] D. Botteldooren, “Finite-difference time-domain simulation of low frequency room acoustic problems,”

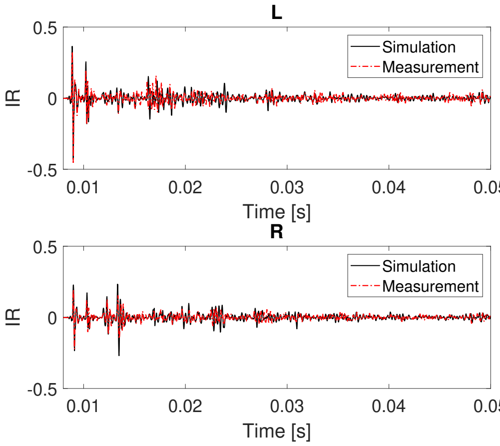

(a) Binaural impulse response.

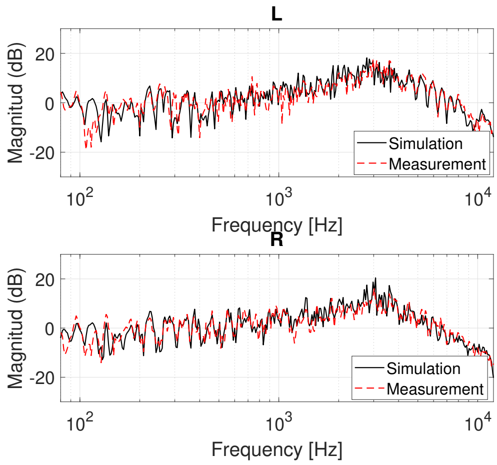

(b) Magnitude in the frequency domain.

Figure 5: Measured and simulated binaural IRs in furnished room using HATS mannequin.

The Journal of the Acoustical Society of America, vol. 98, no. 6, pp. 3302–3308, 1995.

[3] A. Craggs, "A finite element method for free vibration of air in ducts and rooms with absorbing walls," *Journal of Sound and Vibration*, vol. 73, no. 4, pp. 568–576, 1994.

[4] H. Wang, I. Sihar, R. P. Munoz, and M. Hornikx, "Room acoustics modelling in the time-domain with the nodal discontinuous Galerkin method," *The Journal of the Acoustical Society of America.*, vol. 145, no. 4, pp. 2650–2663, 2019.

[5] F. Pind, A. P. Engsig-Karup, C. H. Jeong, J. S. Hesthaven, M. S. Mejling, and J. S. Andersen, "Time domain room acoustic simulations using the spectral element method," *The Journal of the Acoustical Society of America*, vol. 145, no. 6, pp. 3299–3310, 2019.

[6] F. Pind, C.-H. Jeong, A. P. Engsig-Karup, J. S. Hesthaven, and J. Strømann-Andersen., "Time-domain room acoustic simulations with extended-reacting porous absorbers using the discontinuous galerkin method," *The Journal of the Acoustical Society of America*, vol. 148, no. 5, p. 2851–2863, 2020.

[7] H. Wang, M. Cosnefroy, and M. Hornikx, "An arbitrary high-order discontinuous galerkin method with local time-stepping for linear acoustic wave propagation," *The Journal of the Acoustical Society of America*, vol. 149, no. 1, pp. 569–580, 2021.

[8] H. Llopis, A. Engsig-Karup, C.-H. Jeong, F. Pind, and J. Hesthaven, "Reduced basis methods for numerical room acoustic simulations with parameterized boundaries," *The Journal of the Acoustical Society of America*, vol. 152, no. 2, pp. 851–865, 2022.

[9] M. Hornikx and J. Forssén, "A scale model study of parallel urban canyons," *Acustica Acta-Acustica*, vol. 94, no. 2, pp. 265–281, 2008.

[10] ISO, "Acoustics attenuation of sound during propagation outdoors," standard, International Organization for Standardization - ISO/TC 43/SC 2 Building acoustics, 1993.

[11] M. Cosnefroy, S. Gudjónsson, and F. Pind, "Physically accurate binaural reproductions from broadband wave-based room acoustics simulations, and comparison with measurements," in *2023 Immersive and 3D Audio: from Architecture to Automotive (I3DA)*, pp. 1–7, 2023.

[12] ISO, "Acoustics-measurement of room acoustic parameters-part 1: Performance spaces," standard, International Organization for Standardization - ISO/TC 43/SC 2 Building acoustics, June 2009.

[13] T. Komatsu, "Improvement of the Delany-Bazley and Miki models for fibrous sound-absorbing materials," *Acoustical Science and Technology*, vol. 29, no. 1, pp. 121–129, 2008.